

# Description of nucleon scattering on $^{208}\text{Pb}$ by a fully Lane-consistent dispersive spherical optical model potential

W.L. Sun<sup>1,a</sup>, J. Wang<sup>1</sup>, E.Sh. Soukhovitskii<sup>2</sup>, R. Capote<sup>3</sup>, and J.M. Quesada<sup>4</sup>

<sup>1</sup> Institute of Applied Physics and Computational Mathematics, Beijing 100094, China

<sup>2</sup> Joint Institute for Energy and Nuclear Research, Minsk-Sosny 220109, Belarus

<sup>3</sup> Nuclear Data Section, International Atomic Energy Agency, 1400 Vienna, Austria

<sup>4</sup> Departamento de Física Atómica, Molecular y Nuclear, Universidad de Sevilla, Ap. 1065, 41080 Seville, Spain

**Abstract.** A fully Lane-consistent dispersive spherical optical potential is proposed to describe nucleon scattering interaction with doubly magic nucleus  $^{208}\text{Pb}$  up to 200 MeV. The experimental neutron total cross sections, elastically scattered nucleon angular distributions and (p,n) data had been used to search the potential parameters. Good agreement between experiments and the calculations with this potential is observed. Meanwhile, the application of the determined optical potential with the same parameters to neighbouring near magic Pb-Bi isotopes is also examined to show the predictive power of this potential.

## 1. Introduction

Lead-cooled Fast Reactor is thought worldwide as one of the most promising fast neutron system. The European Lead-cooled SYstem (ELSY) project is proposed to investigate the technical and economical feasibility of a high power lead fast reactor [1]. Also a 10 MWt China Lead-based Research reactor (CLEAR-I) is in progress for validation of ADS transmutation system and the Generation-IV reactor [2], where Lead-Bismuth eutectic was selected as primary coolant. Nucleon scattering data of Pb-Bi isotopes with high quality is requested, thus motivated this work to further improve optical model potentials for nuclear data modelling and evaluation.

Various phenomenological optical model potentials for individual nucleus or a group of nuclei had been proposed in the past. An extensively used one is the global spherical optical potential by Koning and Delaroche(K-D) [3] for nucleon-induced reactions up to 200 MeV. However, the conventional optical potentials typically expressed the well depth as a polynomial, meanwhile a number of potential parameters are used for neutron and proton respectively. Recently efforts are given to the applications of dispersive potentials with dispersion relation, such as the dispersive spherical one by Morillon and Romain [4], and the dispersive coupled-channel ones by Soukhovitskii and co-workers [5,6] for actinides and Hao et al. [7] for a mass range of  $A = 24-122$ . The dispersion relation connects the real parts with the imaginary parts of the optical potential, therefore both bound and scattering states are possibly described by the same nuclear mean field as shown in works [8–11]. Also the dispersive constraint helps to reduce the ambiguity and the number of optical potential parameters, and avoids the energy dependent geometry. Correspondingly, the degrees of freedom of the

potential will be reduced substantially, coincident with the request of as few parameters as possible in data analysis.

On the other hand, the charge-exchange (p,n) transitions to the isobar analogue states can be described by the isovector parts of optical potential with an isospin dependence, as discussed by Lane [12,13]. Therefore such (p,n) transitions can be regarded as an additional constraint to potential parameters and a good justification of the isovector parts, as well as a necessary check for the Lane consistency of optical model potential. Approximate Lane consistency of a dispersive coupled-channel optical model(DCCOM) potential has been checked by some of the authors of this work for  $^{232}\text{Th} - ^{238}\text{U}$  [14], and Fe isotopes [15]. Moreover a fully Lane-consistent DCCOM potential is proposed for even Fe isotopes in our previous work [16].

A few dispersive spherical optical potentials had been proposed for magic or near magic nuclei [3,4,17–19]. However they are never fully Lane consistent, since no difference in incident energy for neutron and proton reaching nuclear surface due to Coulomb repulsion had been considered in a consistent approach.

The success of Lane-consistent DCCOM potential for Fe isotopes is very promising, and encourages us to propose a fully Lane consistent dispersive spherical optical potential for magic or near magic nuclei.

Therefore the purpose of this work is to establish such a potential, aimed at justifying it well by analyzing jointly the experimental total cross sections, nucleon angular distributions, as well as (p,n) data. Such a joint analysis can also be thought as a good validation for the Lane consistency of dispersive spherical model potential.

The form of a dispersive optical potential is presented in Sect. 2; the results are compared with measurements, other evaluation and calculation in Sect. 3; finally a summary is given in Sect. 4.

<sup>a</sup> e-mail: sun\_weili@iapcm.ac.cn

## 2. A fully lane-consistent dispersive spherical optical model potential

Based on the DCCOM potential in our previous work [16], a fully Lane-consistent dispersive spherical optical model for Pb-Bi isotopes is expressed as follows:

$$\begin{aligned}
 V(r, E) = & V_{HF}(E^*) \times f_{WS}(r, R_{HF}) \\
 & - [\Delta V_v(E^*) + iW_v(E^*)] \times f_{WS}(r, R_v) \\
 & - [\Delta V_s(E^*) + iW_s(E^*)] \times g_{ws}(r, R_s) \\
 & + \left( \frac{\hbar}{m_\pi c} \right)^2 [V_{SO}(E^*) + \Delta V_{SO}(E^*) \\
 & + iW_{SO}(E^*)] \\
 & \times \frac{1}{r} \frac{d}{dr} f_{WS}(r, R_{SO}) \times (\vec{\sigma} \cdot \vec{L}) \\
 & + V_{Coul}(r, R_c)
 \end{aligned} \quad (1)$$

The geometrical form factors are given as standard Woods–Saxon form. The Coulomb potential  $V_{Coul}(r, R_c)$  is calculated using a spherical one, taking into account the diffuseness of the charge distribution with a charge density form factor equal to  $f_c = [1 + \exp(r - R_c)/a_c]^{-1}$ .

In order to give a identical form of potential for both neutron and proton. Eq. (1) considers an “effective” proton energy,  $E^* = E - C_{Coul}ZZ'/A^{1/3}$ , with account for the Coulomb shift due to the repulsion by nucleus. The constant  $C_{Coul}$ (with the constant  $e^2$  inside) is an free parameter accounting for the “effective” radius of proton interaction in nucleus. Therefore this potential is in a charge-independent form without explicit Coulomb correction terms. Such an account of “effective” proton energy is a generalization of the Coulomb correction with the consideration of full correction in all orders, it is also a pre-condition for this potential to be exactly Lane-consistent [20].

The term  $\Delta V_i(E)$  ( $i = v, s$ ), so-called the dispersive correction term, is determined by the imaginary part  $W(E)$  through the dispersion relation [5–7]:

$$\Delta V(r, E) = \frac{P}{\pi} \int_{-} \frac{W(E')}{E' - E} dE' \quad (2)$$

where the symbol  $P$  denotes the principal value of the integral. The real surface part  $V_s(E)$  is taken only as the dispersive correction term,  $V_s(E) = \Delta V_s(E)$ .

The real spin-orbit term  $V_{so}(E)$  is given as discussed by Walter [21],  $V_{so}(E) = V_{so} e_f^{-\lambda_{so}(E-E)} + \Delta V_{so}(E)$ , where  $V_{so}$  and  $\lambda_{so}$  are free parameters. The dispersive correction term  $\Delta V_{so}(E)$  is also calculated by dispersion relation.

The energy dependences for the imaginary volume term  $W_v(E)$  and imaginary spin-orbit term  $W_{so}(E)$  are adopted as those suggested by Brown and Rho [22]. Same imaginary terms are used in K–D potential also. However the dispersive contribution from imaginary potential to real potential is not considered there. In addition, a modified imaginary potential  $W_v(E)$  was proposed by Soukhovitskii et al. [5, 6] based on the suggestion of Mahaux and Sartor [23], with the consideration of the influence of the non-locality of the imaginary parts. This modified imaginary potential is also used in the present analysis.

The isospin dependence  $(N - Z)/A$  of this potential is considered in the constants:  $A_{HF}$  of real volume  $V_{HF}(E)$  and  $A_s$  of imaginary surface  $W_s(E)$  as follows:

$$A_{HF} = V_0 + (-1)^{Z+1} C_{viso}(N - Z)/A \quad (3)$$

$$A_s = W_0 + (-1)^{Z+1} C_{wiso}(N - Z)/A \quad (4)$$

Therefore the difference between the neutron and proton potentials is identified by the isovector term, Coulomb correction term and Fermi energy, so it is possible to take all the potential parameters to be equal for neutron and proton, while the different parameters for neutron and proton are used in K–D potential, especially for the real parts.

The potential parameters fitting the experimental neutron and proton scattering data are searched by OPTMAN [24] code as usual. This is a code of the coupled-channel optical model based on the soft-rotator or rigid-rotor model. The corresponding coupling form factors, accounting for the coupling strength between ground state(elastic) of target and elastic or excited isobar analogue states of residual nucleus are also implemented into OPTMAN, allowing to directly calculate the quasi-elastic (p,n) data. Since  $^{208}\text{Pb}$  is a double magic nucleus, then other Pb-Bi isotopes must be near magic nuclei. So the option of spherical optical model in OPTMAN is chosen for parameters searching.

A few advantages of this dispersive spherical optical model potential can be summarized as follows:

- (1). Due to the connection of real potential with imaginary potential by dispersion relation, no additional parameters is required, and it is also no need to use the additional polynomial real potential terms as usual. Moreover no energy-dependent geometry (radius and diffuseness) is needed, which will further eliminate the number of free parameters.
- (2). The difference between the neutron and proton potentials is described by the isovector term to real and imaginary potentials. Therefore the isobar analogue state cross section of direct (p,n) scattering can be described, since the (p,n) data are proportional to the isovector terms of potential, and are fixed when the angular distributions are fixed.
- (3). Due to the use of  $A$  and  $Z$  dependent isovector terms, this potential can describe not only one nucleus but also a range of mass number.
- (4). With these isovector terms, the difference between neutron and proton potential is fixed, then both neutron and proton data can be easily described by one potential with same parameters.

The potential parameters involving all isotopes ( $^{206-208}\text{Pb}$  and  $^{209}\text{Bi}$ ) are simultaneously adjusted, as the isovector terms allowed to calculate the data of all mentioned isotopes in one calculation. All of the experimental data are taken from the EXFOR [25] database. Note that the experimental angular distribution data below 5 MeV are not used for parameter searching, as the compound interaction contribution might be important there. That is to say, this work assumed that the nucleon scattering proceeds via direct mechanism only. Also the proton reaction cross sections are not used in such parameters

**Table 1.** Parameters for the dispersive optical model potential. Potential depths are in MeV,  $\lambda_{HF}$ ,  $C_s$ , and  $\lambda_{HF}$  in  $\text{MeV}^{-1}$ , radius and diffuseness in fm.

	Volume	Surface
Real	$V_0 = 52.07 + 0.0292(A-208)$ $\lambda_{HF} = 0.00898$ $C_{viso} = 1.073$	dispersive
Imaginary	$A_v = 12.29, B_v = 81.06$ $E_a = 58$	$W_0 = 17.77, B_s = 12.01$ $C_s = 0.017, C_{viso} = 33.2$
Geometry	$r_{HF} = 1.24 - 0.00066(A-208)$ $a_{HF} = 0.63 + 0.00268(A-208)$ $r_v = 1.2572$ $a_v = 0.69 - 0.00021(A-208)$	$r_s = 1.1817$ $+0.0055(A-208)$ $a_s = 0.628$
	Spin-Orbit	Coulomb
Real	$V_{so} = 7.54$ $\lambda_{so} = 0.005$	$W_0 = 17.77, B_s = 12.01$ $C_s = 0.0175, C_{viso} = 33.2$
Imaginary	$W_{so} = -3.1, B_{so} = 160$	
Geometry	$r_{so} = 1.0792, a_{so} = 0.59$	$r_c = 1.1672, a_c = 0.628$

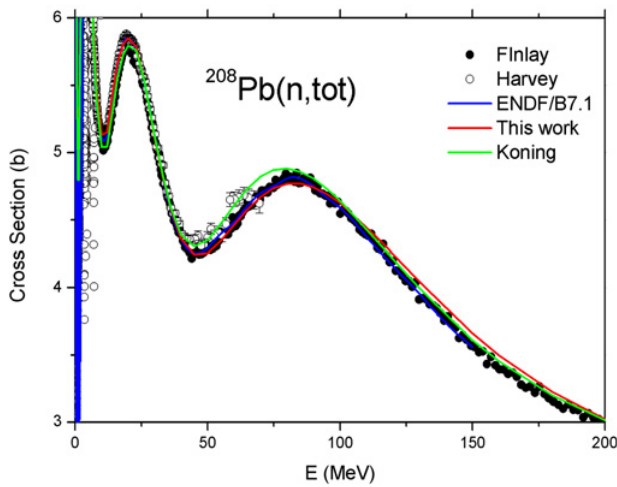


**Figure 1.** Comparison of total cross section for  $^{208}\text{Pb}$  with measurements, ENDF/B7.1, as well as those by K-D potential.

searching. However, different from our previous work [16], (p,n) data are used in this work. The obtained ‘best-fit’ parameters are listed in Table 1.

### 3. Results and discussions

This section shows the results of total neutron cross sections, nucleon elastic angular distributions and (p,n) data for  $^{208}\text{Pb}$  and  $^{209}\text{Bi}$  in order to show the predictive power of the present potential.

Figure 1 shows the neutron total cross sections for  $^{208}\text{Pb}$  up to 200 MeV, compared with experimental data, ENDF/B7.1 evaluation, as well as the results of K-D potential. Good agreement is seen with measurements up to 200 MeV, where ENDF/B7.1 evaluation gives the best agreement, since it is a result fitted to experimental data, and a normalization might be performed. This work agrees with measurements well below 100 MeV, while K-D potential overestimates the data about 1–3% at 50–100 MeV. However, ours overestimated slightly above 100 MeV, while K-D ones are better. The deviation of this work from experimental data is on average within 1–2%, and it is seldom more than 3%.

It is not expected that both potentials reproduce the data very precisely below 5 MeV, since the broad or even

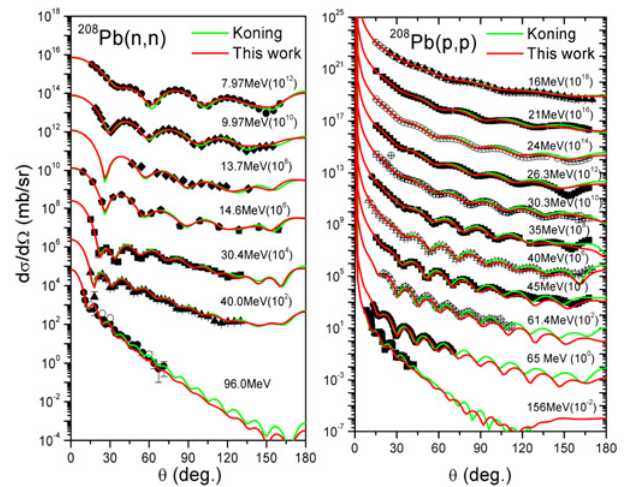


**Figure 2.** Comparison of nucleon elastic angular distributions with measurements for neutron (left) and proton (right), as well as the results of K-D potential.

sharp resonance structures often appear in these lower energy ranges, optical models predict commonly only the average of resonance cross sections.

The predictions of neutron and proton elastic scattering angular distributions for  $^{208}\text{Pb}$  are shown in Fig. 2, respectively, along with the experimental data and those by K-D potential. Obviously for neutron, both predictions describe the data rather well over the whole energy range. For neutron, K-D potential gives slightly better agreement at 96 MeV. For proton, our prediction is almost same as those by K-D potential below 30 MeV, while the latter describes the experimental data slightly better than ours above 30 MeV. In addition, ours show slightly different extrema above 40 MeV.

The results of elastic isobar analog state (IAS) transition cross section of direct (p,n) scattering for  $^{208}\text{Pb}$  is shown in Fig. 3. An overall agreement with measurements is seen for all energies and whole angular region, with the exceptions of slight underestimation at 45 MeV. This demonstrates that our potential gives reasonable parameters for isovector terms.

This potential with same parameters is also applied to  $^{206,207}\text{Pb}$ . The situation of total neutron cross sections, nucleon angular distributions and (p,n) data is quite

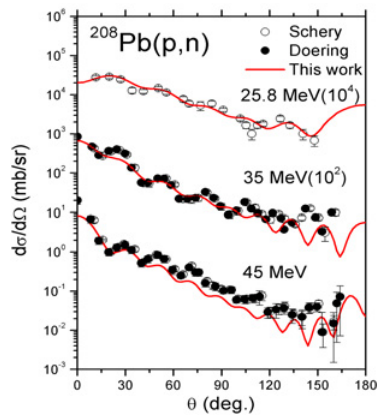


**Figure 3.** Comparison of (p,n) quasi-elastic charge exchange with experimental data for  $^{208}\text{Pb}$ .

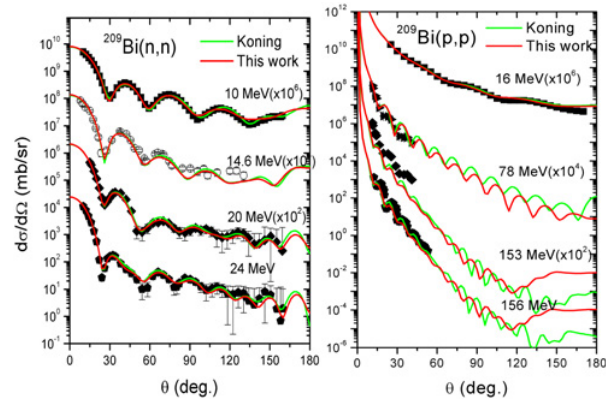


**Figure 5.** Same as Fig. 2, but for  $^{209}\text{Bi}$ .

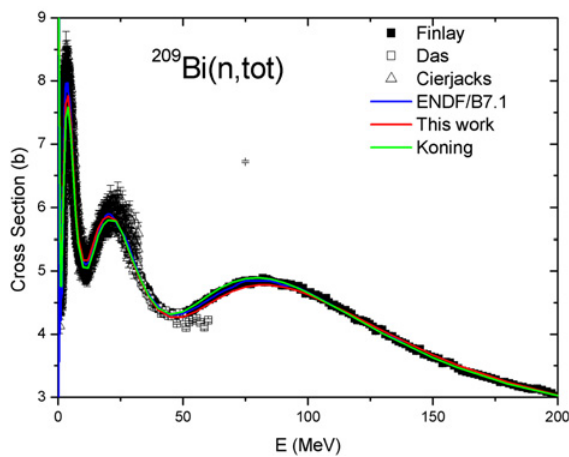


**Figure 4.** Same as Fig. 1, but for  $^{209}\text{Bi}$ .

similar to the situation of  $^{208}\text{Pb}$ . Finally, we present some additional results of  $^{209}\text{Bi}$  in order to show the predictive power for neighboring near magic nuclei.

Figure 4 shows the total cross sections for  $^{209}\text{Bi}$ , compared with measurements, ENDF/B7.1 evaluations and those by K-D potential. Apparently, both potentials give excellent agreement with experimental data. The situation is similar to the case for  $^{208}\text{Pb}$ , however the degree of agreement is even better.

Figure 5 shows the nucleon elastic data for  $^{209}\text{Bi}$ , compared with the measurements and the results of K-D potential. Similar to the case of  $^{208}\text{Pb}$ , both neutron and proton data are well described by both potentials, except for the proton data at 153 MeV, where both potentials underestimate simultaneously the data. However more experimental proton data are necessary to judge further the prediction power.

Similarly the (p,n) data are analyzed and compared with experimental data. The agreement is overall good.

#### 4. Summary

A fully Lane-consistent dispersive spherical optical model potential is proposed for magic or near magic Pb-Bi isotopes, with adjustable parameters identical for both neutron and proton. This potential shows a very good description of available nucleon-nucleus scattering data

up to 200 MeV, including neutron total cross-section and nucleon elastic angular distributions. Additionally, the good prediction for quasi-elastic scattering (p,n) data shows that the isovector components are fixed reasonably, and validates the Lane-consistency of this potential.

This work is partially supported by Project 2015B0103017 of CAEP Science Foundation and Key Laboratory of Neutron Physics of CAEP (Grand No. 2013AA02).

#### References

- [1] L. Cinotti, et al., The Potential of the LFR and the ELSY Project, *Proceedings of the International Congress on Advances in Nuclear Power Plants (ICAPP 2007)*, Nice Acropolis, France, May 13–18
- [2] Y.C. Wu, et al., *Nucl. Sci. and Eng.* **34**, 201 (2014, in Chinese)
- [3] A.J. Koning and J.P. Delaroche, *Nucl. Phys. A* **713**, 231 (2003)
- [4] B. Morillon, et al., *Phys. Rev. C* **70**, 014601 (2004)
- [5] E.Sh. Soukhovitskiĭ, R. Capote, J.M. Quesada et al., *Phys. Rev. C* **72**, 024604 (2005)
- [6] R. Capote, E.Sh. Soukhovitskiĭ, J.M. Quesada et al., *Phys. Rev. C* **72**, 064610 (2005)
- [7] Lijuan Hao, Weili Sun and E. Sh. Soukhovitskiĭ, *J. Phys. G: Nucl. Part. Phys.* **35**, 095103 (2008)
- [8] B. Morillon and P. Romain, *Phys. Rev. C* **74**, 014601 (2006)
- [9] O.V. Bespalova, et al., *Bull. Russ. Acad. Sc. Phys.* **71**, 428 (2007)
- [10] *Bull. Russ. Acad. Sc. Phys.* **73**, 816 (2009)
- [11] W.H. Dickhoff, et al., *Phys. Rev. C* **82**, 054306 (2010)
- [12] A.M. Lane, *Phys. Rev. Lett.* **8**, 171 (1962)
- [13] A.M. Lane, *Nucl. Phys.* **35**, 676 (1962)
- [14] J.M. Quesada, R. Capote, E.Sh. Soukhovitskiĭ, S. Chiba, *Phys. Rev. C* **76**, 057602 (2007)
- [15] R. Li, W. Sun, E.Sh. Soukhovitskiĭ et al., *Phys. Rev. C* **87**, 054611 (2013)
- [16] W. Sun, R. Li, E.Sh. Soukhovitskiĭ et al., *Nucl. Data Sheets* **118**, 191 (2014)
- [17] W. Tornow W, et al., *Phys. Rev. C* **42**, 693 (1990)
- [18] G.J. Weisel, et al., *Phys. Rev. C* **54**, 2410 (1996)
- [19] C. Mahaux, et al., *Nucl. Phys. A* **528**, 253 (1991)
- [20] R. Capote, E.Sh. Soukhovitskiĭ, *Int' Conf. on Nucl. Data for Sci. and Tech.*, 239 (2007)

- [21] R.L. Walter *Proc. Meeting on Nucleon–Nucleus Optical Model up to 200 MeV* (France: Bruyères-le-Châtel), **199** (1996)
- [22] G.E. Brown et al., *Nucl. Phys. A* **372**, 397 (1981)
- [23] C. Mahaux et al., *Nucl. Phys. A* **528**, 253 (1991)
- [24] E.Sh. Soukhovitskii et al., Report JEARI-Data/Code 2005-002(2005), Supplement to OPTMAN code manual Version 10 (2008)
- [25] EXchange FORmat database(EXFOR). Available online at <http://www-nds.iaea.org/exfor>